Contents lists available at ScienceDirect

Nuclear Instruments and Methods in Physics Research B

Experimental approach and atomistic simulations to investigate the radiation tolerance of complex oxides: Application to the amorphization of pyrochlores

G. Sattonnay [a],*, L. Thomé [b], N. Sellami [a], I. Monnet [c], C. Grygiel [c], C. Legros [a], R. Tetot [a]

[a] Univ. Paris Sud, ICMMO-LEMHE, Bât. 410, F-91405 Orsay, France
[b] CSNSM, CNRS, IN2P3, Université Paris-Sud, Bât. 108, F-91405 Orsay, France
[c] CIMAP, CEA, CNRS, Université de Caen, BP 5133, F-14070 Caen Cedex 5, France

A B S T R A C T

Both experimental approach and atomistic simulations are performed in order to investigate the influence of the composition of pyrochlores on their radiation tolerance. Therefore, $Gd_2Ti_2O_7$ and $Gd_2Zr_2O_7$ were irradiated with 4 MeV Au and 92 MeV Xe ions in order to study the structural changes induced by low and high-energy irradiations. XRD results show that, for both irradiations, the structural modifications are strongly dependent on the sample composition: $Gd_2Ti_2O_7$ is readily amorphized, whereas $Gd_2Zr_2O_7$ is transformed into a radiation-resistant anion-deficient fluorite structure. Using atomistic simulations with new interatomic potentials derived from the SMTB-Q model, the lattice properties and the defect formation energies were calculated in $Gd_2Ti_2O_7$ and $Gd_2Zr_2O_7$. Calculations show that titanates have a more covalent character than zirconates. Moreover, in $Gd_2Ti_2O_7$ the formation of cation antisite defects leads to strong local distortions around Ti-defects and to a decrease of the Ti coordination number, which are not observed in $Gd_2Zr_2O_7$. Thus, the radiation resistance is related to the defect stability: the accumulation of structural distortions around Ti-defects could drive the $Gd_2Ti_2O_7$ amorphization induced by irradiation.

© 2014 Elsevier B.V. All rights reserved.

1. Introduction

Understanding the behavior of complex oxides submitted to ion irradiation is crucial in order to predict their radiation tolerance, to establish criteria controlling their structural stability and to identify relevant factors for the occurrence of phase transformations. Among complex oxides, pyrochlores with the $A_2B_2O_7$ stoichiometry were thoroughly investigated during the last decades, due to the large array of structural and physical properties related to their chemical compositions [1]. For instance, pyrochlores were considered as potential immobilization matrices for actinides produced in nuclear power plants, due to their ability to incorporate these species (e.g. U, Np, Th, Pu, Am and Cm) which are generated through the reprocessing of spent fuel arising from nuclear reactors [2].

Ordered $A_2B_2O_7$ pyrochlores belong to the Fd$\overline{3}$m space group which is a superstructure of the ideal fluorite structure (Fm$\overline{3}$m space group) with twice the lattice constant. A and B cations occupy the 16c (0, 0, 0) and 16d (0.5, 0.5, 0.5) sites, respectively,

and oxygens are located at the 48f (x, 0.125, 0.125) and 8b (0.375, 0.375, 0.375) positions (using wyckoff notation). The anion sublattice can be completed by adding missing oxygens in the 8a site to form the fluorite structure. Geometrically, A cations are coordinated to six 48f oxygens and two 8b oxygens, whereas B cations are six-coordinated to 48f oxygens. The stability of the pyrochlore structure is governed by the ratio of the ionic radii of A and B cations (r_A/r_B) which extends from 1.46 for $Gd_2Zr_2O_7$ to 1.78 for $Sm_2Ti_2O_7$ [1,3].

Defects in insulators crucially determine their physical, chemical and electronic properties. Understanding and controlling the defect formation in complex structures is thus essential, particularly for those employed in extreme environments where defects may prevail. In particular, the radiation resistance of pyrochlores seems to be correlated to the defect stability and/or the structural disordering [4]. For instance, in the $Gd_2(Ti_xZr_{(1-x)})_2O_7$ family, it has been reported that the susceptibility to radiation-induced amorphization exhibits a systematic decrease with increasing Zr content. Whereas $Gd_2Ti_2O_7$ is readily amorphized, the end member $Gd_2Zr_2O_7$ is transformed into a radiation resistant anion-deficient fluorite structure upon irradiation at room temperature [5–19]. From these results, it was concluded that zirconates are more

* Corresponding author. Tel.: +33 1 69 15 70 37.
  E-mail address: gael.sattonnay@u-psud.fr (G. Sattonnay).

radiation resistant than titanates, and that ion-beam induced amorphization increases with increasing B-site cation size from $Gd_2Ti_2O_7$ to $Gd_2Zr_2O_7$. Nevertheless, it is now believed that the radiation response cannot be described exclusively in terms of the cationic radius ratio: the defect-formation energies and the bond type (i.e. the electronic structure of compounds) must be considered [3,9,20]. It has been suggested that the resistance of materials to amorphization in a complex non-metallic compound is determined by a competition between short-range covalent interactions and long-range ionic forces. However, it is not easy to quantify the covalency and ionicity of materials and to relate these parameters to their radiation resistance. Despite a high number of experimental and theoretical works devoted to the study of the process of radiation induced amorphization in pyrochlores, the underlying mechanisms are not yet well understood.

This paper reports a comparative study of the damage created by heavy ions in $Gd_2Ti_2O_7$ and $Gd_2Zr_2O_7$ in order to investigate the effects of the chemical composition on the radiation resistance. X-ray diffraction (XRD) was implemented to determine the structural changes induced by irradiation. Moreover, in an attempt to explain some experimental observations concerning the radiation resistance of pyrochlores as a function of their composition, atomistic simulations of Gd_2Ti_2O7 and $Gd_2Zr_2O_7$ were performed using a new variable-charge model (the so-called SMTB-Q model, Second-Moment Tight-Binding-QEq) [21–23]. This model takes advantage of an oxygen-metal interatomic potential which better describes the iono-covalent bonding of oxides than classical purely ionic potentials. It was used in the present work to determine the role played by the defect stability on the radiation tolerance of pyrochlores and to try to elucidate the mechanisms governing the structural stability of these compounds under irradiation.

2. Experimental results

2.1. Experimental procedure

Polycrystalline pyrochlore pellets were prepared by a standard solid state process. Stoichiometric amounts of A_2O_3 and BO_2 oxides were intimately mixed in an acetone slurry using a ball-mill and subsequently dried. After drying, the powders were isostatically pressed into rods at 250 MPa. The homogenized mixtures were then subjected to a three step heating protocol with intermittent grindings to attain a better homogeneity. The compacts were first sintered at 1200 °C for 12 h. The procedures (grinding, milling, pressing) were repeated twice with a second heating at 1400 °C for 72 h and a final sintering in air at 1450 °C for 196 h in order to increase the density of samples. Pellets were cut with a diamond saw and the specimens were polished to a 0.5 μm diamond finish.

Pyrochlore oxides were irradiated at room temperature with 4 MeV Au ions (LE) at the JANNUS accelerator of the CSNSM in Orsay at fluences ranging from 10^{12} up to 10^{16} cm^{-2}, and with 92 MeV Xe ions (HE) at the GANIL accelerator in Caen at fluences ranging from 2.5×10^{11} to 10^{14} cm^{-2}. Table 1 summarizes the values of the projected ion ranges (R_p), nuclear (S_n) and electronic (S_e) stopping powers computed with the SRIM code [24] for the

various irradiations (these values depend slightly on the sample composition). It is worth noting that S_n is negligible as compared to S_e for HE irradiations, whereas S_n and S_e are of the same order of magnitude for LE irradiations.

XRD experiments were performed with a X'pert Pro MRD PANalytical diffractometer, using a Cu$_{K\alpha}$ anticathode ($\lambda_{K\alpha1}$ = 0.1540598 nm, $\lambda_{K\alpha2}$ = 0.1544426 nm). X-ray patterns were recorded in a standard ($\theta-2\theta$) geometry in a 13°–90° range (2θ) with a step of 0.025°. For LE irradiations a grazing incidence of 2° was used.

2.2. XRD results

Fig. 1 shows XRD patterns recorded on $Gd_2Ti_2O_7$ and $Gd_2Zr_2O_7$ irradiated with LE (Fig. 1) and HE (Fig. 2) ions. For $Gd_2Ti_2O_7$ a progressive vanishing of all diffraction peaks is observed at increasing fluence and an additional diffuse scattering occurs at the basis of the (2 2 2) pyrochlore peak (at $2\theta\sim30°$, Figs. 1a and 2a). These features indicate that both LE and HE irradiations lead to the amorphization of samples. Conversely, for $Gd_2Zr_2O_7$ the diffraction

Table 1
Ion energy (E), ion projected range (R_p), nuclear (S_n) and electronic (S_e) stopping powers calculated with the SRIM code [18] for the different ions used in this work.

Ion	E (MeV)	R_p (μm)	S_e (keV/nm)[a]	S_n (keV/nm)[a]
Au	4	0.5	3.3	5.0
Xe	92	8.3	20	0.4

[a] Maximum values obtained in the depth range probed by XRD (≈3 μm in a standard geometry, ≈500 nm in a grazing incidence of 2°).
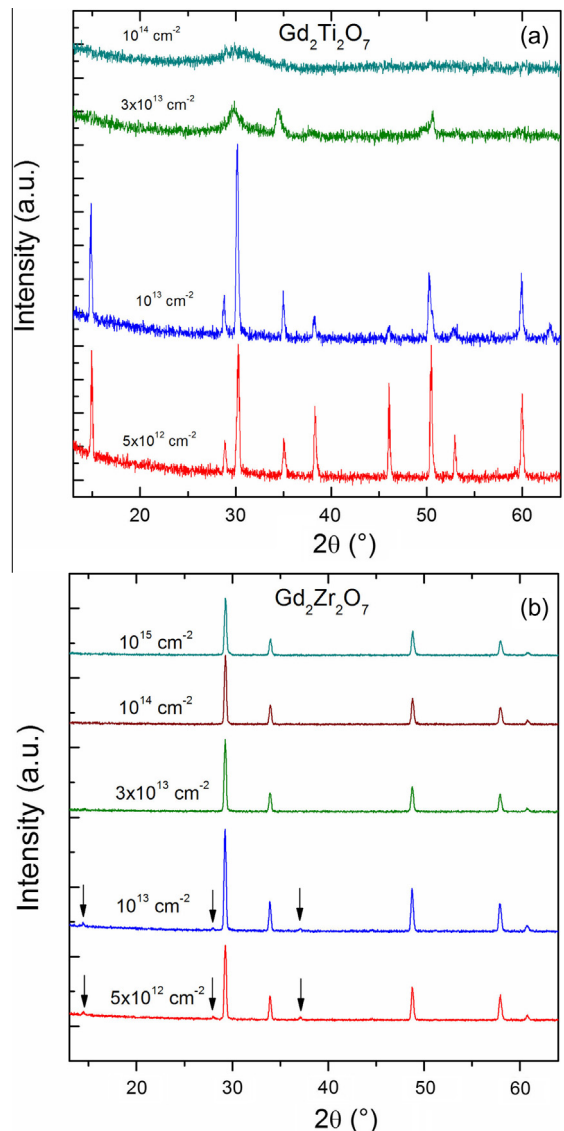
Fig. 1. XRD patterns recorded on $Gd_2Ti_2O_7$ (a) and $Gd_2Zr_2O_7$ (b) before and after irradiation with 4-MeV Au ions at increasing fluences.